

Optimal control of tidal barrages considering economic factors

Agustina Skiarski, Nicolás Faedo, and John V. Ringwood

Abstract—Tidal barrage power plants generate power by virtue of the variations of the tidal elevation throughout the day. A tidal barrage consist of a dam, with turbines and sluice gates, that separates an inner basin from the sea, creating a hydraulic head between the inner basin water level and the sea water level. This head drives water through the turbines, transforming potential energy into mechanical (and subsequently electrical) energy. Given the mass of water contained within the basin, added to the slow dynamics of the tidal elevation, tidal barrages can be used as variable storage facilities. This provides flexibility to their operation, which can be exploited to shift the generation periods of the turbines present in the tidal barrage. As a result, the power generation profile can be adjusted to maximise output during hours when electricity prices are high. In this paper, we explore different objective functions to optimally operate the turbines and sluice gates of a tidal barrage, using a model based on the La Rance power plant. The aim is to include wholesale electricity prices, as well as estimated operational costs, in the objective function of tidal barrage operation, and analyse how these considerations impact overall energy generation, timing of power output, and pumping requirements.

Index Terms—Tidal barrages, optimal control, energy prices, economic analysis.

I. INTRODUCTION

TIDAL barrages are a type of ocean energy power plant that generate electricity by virtue of the daily tidal level variations in the sea. In these power plants, an embankment, located in a coastline or estuary, separates the open sea from a basin, creating a head difference between the basin water level and the tidal water level. Turbines located along the embankment allow the basin to fill and empty as the external tidal water level changes, transforming potential energy into mechanical, and subsequently electrical, energy. Additionally, the embankment has sluice gates that can be opened and closed to increase the flow through the barrage and effectively control the operating head. Tidal barrages can be operated with more flexibility compared to other more traditional renewable plants (such as solar and wind power plants) because of the variable energy storage capacity of the basin. Moreover, the turbines can be operated in pumping

mode to increase the available head during generation periods with a net increase in power output, which gives tidal barrages capabilities somewhat similar to pumped storage plants. As a results, the generating periods of tidal barrages, withing certain limits, can be timed according to different control objectives [1].

Apart from the traditional energy maximising (EM) approach seen in the literature for tidal barrage operational optimisation, income maximising (IM) objective functions have been explored in tidal barrage optimal control, where hourly electricity prices are considered, in order to shift generation periods of the turbines to hours where energy prices are high. For instance, [2], [3] compare the operation of a tidal barrage resulting from using both EM and IM objectives, where the control variables are the timing of generation and pumping periods. Another example of implementing an IM objective is [4], where the number of operating turbines is optimised, considering a linearised tidal barrage model. On the other hand, [5] introduces a revenue maximising objective funtion, where the number of operating turbines is controlled by including OpEx into the objective function, assuming a constant cost (in £/MW/h) for every hour of operation of each turbine. Although this is a rather simplified calculation for turbine OpEx, it does qualitatively reflect the cost of having the turbines in service, as turbine OpEx increases with operational duration [6].

This study presents a comparison between EM and IM objective functions to optimise tidal barrage operation, where the optimal control problem (OCP) for tidal barrages is formulated so that the turbine flows and sluice gate areas are controlled, which allows more flexibility in the control solution, compared to previous approaches. The goal is to show the impact of different objective functions on power plant income, energy generation, and pumping periods of the turbines. Moreover, by means of a novel control allocation algorithm, the number of operating turbines is computed to estimate OpEx, and evaluate if the change in objective function results in a more costly operation. Because continuous-time optimal control problems for tidal barrages are infinite-dimensional, moment-based control [7], [8] is implemented to discretise the control problem and solve for the optimal trajectories. Moment-based control has been shown [9] to be a computationally effective tool to solve the tidal barrages OCP by capturing the harmonic nature of the tidal elevation in order to parameterise the control and state variables.

The reminder of this paper is organised as follows: Section II presents the tidal barrage model used for

© 2025 European Wave and Tidal Energy Conference. This paper has been subjected to single-blind peer review.

Agustina Skiarski is grateful for support of Taighde Éireann – Research Ireland under Grant number 18/CRT/6049. For the purpose of Open Access, the author has applied a CC BY public copyright licence to any Author Accepted Manuscript version arising from this submission.

John Ringwood was supported by the Marine Renewable Ireland (MaREI) Centre under Grant No. 12/RC/2302_P2.

Digital Object Identifier:

<https://doi.org/10.36688/ewtec-2025-963>

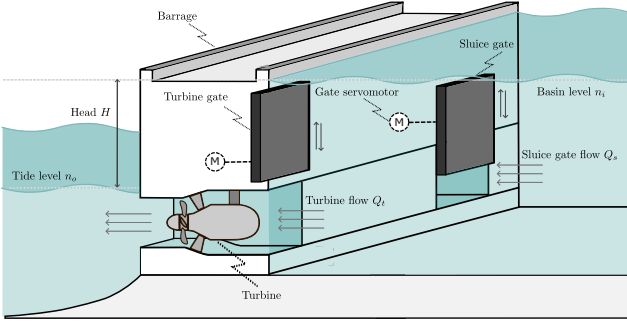


Fig. 1. Schematic diagram of a tidal barrage

TABLE I
PARAMETERISATION OF THE TIDAL BARRAGE MODEL,
BASED ON LA RANCE POWER PLANT [10]

Parameter	Value	Unit
Maximum sluice gate area A_s^{max}	900	m ²
Sluice discharge coefficient C_{ds}	1	-
Number of turbines n	24	-
Turbines rated power P_{max}	10	MW
Maximum turbine flow Q_t^{max}	260	m ³ /s
Maximum inner basin level N_i^{max}	5	m

control calculations, while Section III outlines the OCP for tidal barrages, the moment-based parameterisation used to solve the OCP, and the different objective functions used. In Section IV, the solutions of the OCP are presented, as well as the OpEx calculations using the control allocation algorithm. Conclusions are drawn in Section V.

II. TIDAL BARRAGE MODEL

In this section, the tidal barrage model used in this study is presented. The model is based on the La Rance power plant, located in St. Malo, France, which is the first large-scale commercial tidal barrage constructed, with an installed capacity of 240 MW. Table I shows the parameterisation of the tidal barrage model adopted in this study. A representation of a tidal barrage is shown in Figure 1.

A. Tidal elevation

The ocean tidal water level can be represented as the sum of harmonic functions, or tidal *constituents*, where each function is associated with a particular astronomic phenomena. In this paper, the tidal elevation at the site where La Rance is located is reconstructed using the EOT20 global tidal model [11]. The EOT20 model provides amplitudes and phases for 17 astronomic constituents around the world, with a spatial resolution of 0.125 degrees, which allows reconstruction of the water level during a certain period of time and for a particular location.

B. Hydrodynamic model

Assuming a simplified zero-dimensional (0D) model [12], the rate of change in the basin inner level is

proportional to the net water flow that enters and leaves the basin:

$$A_b(n_i(t))\dot{n}_i(t) = -Q_t(t) - Q_s(t), \quad (1)$$

where $A_b(n_i(t)) \in \mathbb{R}$ is the wetted surface area inside the basin, $n_i(t) \in \mathbb{R}$ is the inner basin level, $Q_t(t) \in \mathbb{R}$ is the total flow through the turbines, and $Q_s(t) \in \mathbb{R}$ is the flow through the sluice gates. Note that the area A_b is a function of the inner basin level, to account for the irregular topology of the estuary where the barrage is located. In this study, A_b is assumed to vary linearly with n_i , based on the model used in [10].

C. Hydraulic turbines

The instantaneous power $p_t^i(t)$ generated by the i^{th} hydraulic turbine in the barrage is calculated as:

$$p_t^i(t) = \rho g \eta(H(t), q_t^i(t)) H(t) q_t^i(t), \quad (2)$$

where ρ is the water density, g is gravitational acceleration, q_t^i is the flow through the i^{th} turbine, $\eta(H, q_t^i)$ is the efficiency of the i^{th} turbine, and H is the hydraulic head, *i.e.*:

$$H(t) = n_i(t) - n_o(t). \quad (3)$$

The total power generated by the tidal barrage plant is computed by summing the instantaneous power in Equation (2):

$$P_t(t) = \sum_i^n p_t^i(t), \quad (4)$$

n being the number of turbines in the barrage. The extracted energy over an interval $\Omega = [0, T] \subset \mathbb{R}^+$ is:

$$E_t(t) = \int_{\Omega} P_t(t) dt. \quad (5)$$

Note that the total water flow through the turbines, $Q_t(t)$ in Equation (1), is:

$$Q_t(t) = \sum_i^n q_t^i(t). \quad (6)$$

For controller calculations, the tidal barrage model assumes that all the turbine operate equally at the same flow q_t . The efficiency of the turbines, η , is given by the turbine hill chart [13], a static map of the operating points of the turbine created by the manufacturer. In this study, η is extracted from the hill chart for each pair (H, q_t) , as in [8].

D. Sluice gate

The flow through the sluice gates is defined by:

$$Q_s(t) = C_{ds} \text{sign}(H(t)) \sqrt{2g|H(t)|} A_s(t), \quad (7)$$

where C_{ds} is the coefficient of discharge for a sluice gate. Equation (7) shows that the sluice gate flow can be controlled via the sluice gate opening area $A_s(t)$.

III. OPTIMAL CONTROL PROBLEM FORMULATION

The optimal control problem (OCP), associated with tidal barrage operation presented in this study, consists of finding an optimal trajectory for the flow through the turbines $Q_t(t)$ and the total sluice gate area $A_s(t)$ (which controls the flow through the sluice gates), to maximise an objective function \mathcal{J} :

$$\begin{aligned} (Q_t^{\text{opt}}, A_s^{\text{opt}}) &= \arg \max_{(Q_t, A_s)} \mathcal{J}(n_i, Q_t, A_s), \\ \text{subject to:} \\ \dot{n}_i &= f(n_i, Q_t, A_s), \\ |n_i| &\leq N_i^{\text{max}} \quad (\text{basin water level limits}), \\ |Q_t| &\leq Q_t^{\text{max}} \quad (\text{turbine flow limits}), \\ 0 \leq A_s &\leq A_s^{\text{max}} \quad (\text{sluice gate opening limits}), \\ |P_t| &\leq P_{\text{max}} \quad (\text{turbine power limits}). \end{aligned} \quad (8)$$

where $f(\cdot)$ is the mapping that defines the dynamics of the system, as per Equation (1).

A. Moment-based control

Here, the moment-based parameterisation used to solve the tidal barrage OCP is briefly recalled. The discretisation of the tidal barrage OCP using moments, previously used in [7]–[9], is based on the definition of a signal generator, whereby both controllable and uncontrollable inputs affecting the tidal barrage system can be parameterised, similarly to spectral weighted residual methods [14]. Because of the periodic nature of the tidal elevation, the signal generator used in this study is such that it generates a family of harmonic functions used to map the tidal level $n_o(t)$, as well as the control pair $(Q_t(t), A_s(t))$:

$$\begin{aligned} \dot{\theta}(t) &= S\theta(t), \\ n_o(t) &= L_{n_o}\theta(t), \\ Q_t(t) &= L_{Q_t}\theta(t), \\ A_s(t) &= L_{A_s}\theta(t), \end{aligned} \quad (9)$$

with

$$S = 0 \oplus \left(\bigoplus_{p=1}^d \begin{bmatrix} 0 & p\omega_0 \\ -p\omega_0 & 0 \end{bmatrix} \right), \theta(t) = \begin{bmatrix} 1 \\ \cos \omega_0 t \\ \sin \omega_0 t \\ \dots \\ \cos \omega_0 t \\ \sin \omega_0 t \\ \dots \\ \cos d\omega_0 t \\ \sin d\omega_0 t \end{bmatrix}, \quad (10)$$

where $\theta(t) \in \mathbb{R}^\nu$, $\{L_{n_o}^\top, L_{Q_t}^\top, L_{A_s}^\top\} \in \mathbb{R}^\nu$, $\nu = 2d + 1$, $\omega_0 = \frac{2\pi}{T}$ is the fundamental frequency, and d is the number of harmonics of ω_0 included in the signal description. The resulting frequencies in the signal generator are such that the matrix S has *simple* (i.e. no repeated) eigenvalues, to guarantee that the OCP is well-posed [15]. Suppose that the initial condition of the signal generator $\theta(0)$ is such that the pair $(S, \theta(0))$ is reachable. Then, the moment of the system, defined as:

$$\frac{\partial \pi(\theta(t))}{\partial \theta(t)} S\theta(t) = f(\pi(\theta(t)), L_{Q_t}\theta(t), L_{A_s}\theta(t)), \quad (11)$$

can be approximated, with d sufficiently large, as:

$$\pi(\theta(t)) \approx L_{n_i}\theta(t), \quad (12)$$

where $L_{n_i}^\top \in \mathbb{R}^\nu$. Hence, for any given trajectory $\theta(t)$, the steady state response of the system can be approximated as:

$$n_i^{\text{ss}}(t) \approx L_{n_i}\theta(t), \quad (13)$$

with

$$\dot{n}_i(t) = L_{n_i}\dot{\theta}(t) = L_{n_i}S\theta(t). \quad (14)$$

L_{n_i} can then be computed with a collocation method [16] by defining the following residual function \mathcal{R} :

$$\begin{aligned} \mathcal{R}(L_{n_i}, L_{Q_t}, L_{A_s}, t) &= \\ &A_b(L_{n_i}\theta(t))L_{n_i}S\theta(t) + L_{Q_t}\theta(t) + \\ &C_{ds}L_{A_s}\theta(t)\sqrt{2g(L_{n_i} - L_{n_o})\theta(t)}, \end{aligned} \quad (15)$$

and forcing \mathcal{R} to be 0 at a finite set of *time collocation points* $N_c \in \mathbb{N}$. The time collocation results in the following non-linear system of equations:

$$R(L_{n_i}, L_{Q_t}, L_{A_s}) = \begin{bmatrix} \mathcal{R}(L_{n_i}, L_{Q_t}, L_{A_s}, t_{N_1}) \\ \vdots \\ \mathcal{R}(L_{n_i}, L_{Q_t}, L_{A_s}, t_{N_c}) \end{bmatrix} = 0. \quad (16)$$

The resulting constrained OCP, for tidal barrage operation in the moment-domain, can be written as follows:

$$\begin{aligned} (L_{Q_t}^{\text{opt}}, L_{A_s}^{\text{opt}}) &= \arg \max_{(L_{Q_t}, L_{A_s})} \mathcal{J}(L_{n_i}, L_{Q_t}, L_{A_s}), \\ \text{subject to:} \\ R(L_{n_i}, L_{Q_t}, L_{A_s}) &= 0, \\ L_{n_i}\mathcal{A} &\leq \mathcal{B}_{n_i}, \\ L_{Q_t}\mathcal{A} &\leq \mathcal{B}_{Q_t}, \\ L_{A_s}\mathcal{A} &\leq \mathcal{B}_{A_s}, \\ \rho g \mathcal{M} \odot (L_{n_i} - L_{n_o})\mathcal{A} &\odot (L_{Q_t}\mathcal{A}) \leq \mathcal{B}_{P_t}, \end{aligned} \quad (17)$$

where

$$\begin{aligned} \Lambda &= [\theta(t_{N_1}) \quad \dots \quad \theta(t_{N_c})], \\ \mathcal{A} &= [\Lambda \quad \Lambda], \\ \mathcal{B}_{n_i} &= [N_i^{\text{max}}\mathbf{1}_{N_c} \quad -N_i^{\text{max}}\mathbf{1}_{N_c}], \\ \mathcal{B}_{Q_t} &= [Q_t^{\text{max}}\mathbf{1}_{N_c} \quad -Q_t^{\text{max}}\mathbf{1}_{N_c}], \\ \mathcal{B}_{A_s} &= [A_s^{\text{max}}\mathbf{1}_{N_c} \quad \mathbf{0}_{N_c}], \\ \mathcal{B}_{P_t} &= [P_{\text{max}}\mathbf{1}_{N_c} \quad -P_{\text{max}}\mathbf{1}_{N_c}]. \end{aligned} \quad (18)$$

B. Objective functions

Two different objective functions are considered in this study: energy maximisation (EM) and income maximisation (IM), described in this section. A relevant assumption is that the controller has perfect information of the external inputs, *i.e.* the tidal elevation and wholesale electricity prices.

1) *Energy maximisation (EM)*: Under an EM objective, the purpose is to maximise energy generation over Ω :

$$\mathcal{J}_{EM} := \int_{\Omega} P_t dt, \quad (19)$$

where the power is calculated in the moment-domain parameterisation as:

$$P_t = \rho g \eta (L_{n_i} - L_{n_o}) \theta (L_{Q_t} \theta)^T. \quad (20)$$

2) *Income maximisation (IM)*: With an IM objective, the goal is to maximise the income of the power plant, which is a function of the hourly wholesale electricity price $p(t)$:

$$\mathcal{J}_{IM} := \int_{\Omega} p \times P_t dt. \quad (21)$$

The electricity price values $p(t)$ used in this study are extracted from [17], and shown in Figures 2 and 3. The time series $p(t)$ is used to cost the electricity consumed during pumping, as well as the generated power.

IV. RESULTS

In order to assess the performance of the controller with the different objective functions, two cases are presented: a winter case, spanning January 23rd 2023 to February 21st 2023, and a summer case, spanning June 30th to July 29th. Both periods are chosen so as to include a full lunar cycle in each case, and to represent different energy market price behaviour, thus covering a comprehensive set of external inputs. As shown in Figures 2 and 3, the tidal resource varies slightly in terms of maximum amplitude, in both cases, although, during the winter period illustrated, there is a larger difference between spring and neap tide amplitudes. The largest discrepancy, however, is seen in the energy prices: the mean electricity price during the winter case is 155 Euro/MWh while, during the summer period illustrated, the mean electricity price is 79 Euro/MWh. Moreover, while winter prices vary in a range between 90 Euro/MWh and 250 Euro/MWh, summer prices achieve negative values during 43 hours, with a negative peak of -135 Euro/MWh¹.

A. Optimal control solutions

Table II shows the results of a winter and summer scenario. Generation is the positive output energy from the power plant, while pumping is the negative energy consumed by the power plant. As expected, the EM objective function results in a higher energy generation compared to the IM objective. In the winter case, the IM objective results in lower pumping requirements, *i.e.* the controller tries to reduce the cost of consuming energy from the grid. On the other hand, in the summer case, the pumping requirements increase when implementing the IM objective, evidencing the efforts of the controller to shift the generation periods due to the substantial difference in price range during the

¹Negative prices are due to a surplus of generating capacity on the grid, with the French system heavily supported by (relatively inflexible) nuclear generation.

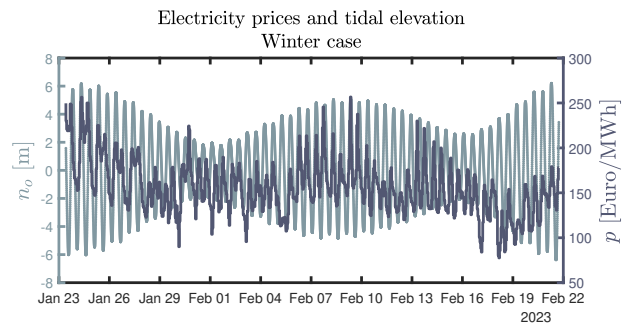


Fig. 2. External inputs used in the winter case: tidal water elevation (left axis) and electricity prices (right axis).

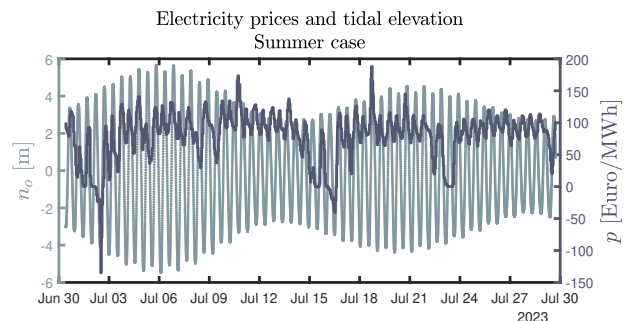


Fig. 3. External inputs used in the summer case: tidal water elevation (left axis) and electricity prices (right axis).

TABLE II
ENERGY AND INCOME FOR WINTER AND SUMMER PERIODS

Parameter	Winter period		Summer period	
	EM	IM	EM	IM
Generation [GWh]	59.6	57.4	53.3	47.1
Pumping [GWh]	-28.2	-26.2	-25.7	-29.4
Income [k Euro]	9,325	9,114	3,919	4,103

chosen summer period. It is particularly interesting, in the summer case, that the IM objective results in a reduction of almost 12% in energy generation with respect to the EM objective, but with an increase of almost 6% in income.

Figure 4 shows the power generated with the control solutions of the two objective functions in the summer case for a 30 hour period (orange lines), against the hourly electricity prices (black line). It can be seen that the solution with an the IM objective (dashed line) is such that, during hours with negative prices, the power plant is pumping, as opposed to the solution of the EM objective (bold line) where the power plant generates at full capacity. Furthermore, although the generation periods resulting from the IM objective do not exactly coincide with peak electricity prices, it shown that, for instance, between hours 55 and 60, the generation period with the IM objective is extended, compared to generation with the EM objective. Note that, in this study, the IM objective assumes that energy consumed during pumping is priced with the wholesale electricity prices, meaning that pumping during hours where the electricity prices are negative results in an income for the power plant. Even though this might not be the case in reality, from a power system operation perspec-

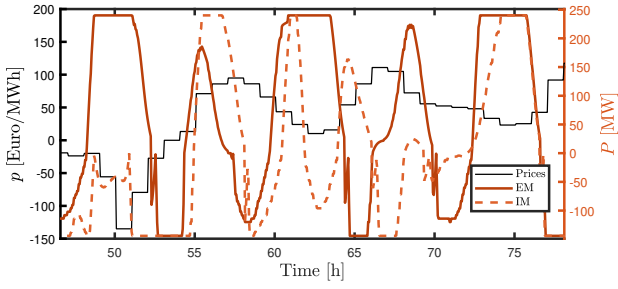


Fig. 4. Electricity prices (black line, left axis) and power generation (orange lines, right axis) resulting from the optimal control solutions, using the two different objective functions: EM (bold line) and IM (dashed line).

tive, it is indeed desirable to consume electricity during hours of negative prices during which generation from traditional renewable sources (*i.e.* solar and wind) is higher than the demand. The (time varying) energy storage facility characteristic of tidal barrages can be used to avail of such negative price scenarios.

B. Calculation of number of operating turbines and OpEx

Although it is shown in Section IV-A that the IM objective function increases the income of the power plant compared to the EM objective function, it is of interest to study if operating the tidal plant with an IM objective function results in more costly operation of the turbines. With this in mind, in order to approximate the OpEx associated with turbine operation, a control allocation algorithm is presented to calculate the number of operating turbines at each instant $n_{op}(t)$:

$$n_{op}(t) = \text{card}(\mathcal{N}), \quad (22)$$

where $\text{card}(\mathcal{N})$ denotes the cardinal number of the set \mathcal{N} , defined as:

$$\mathcal{N} = \{i \in \{1, \dots, n\} \subset \mathbb{N} | q_t^i(t) \neq 0\}. \quad (23)$$

Following the model used in [13], based on the turbine hill chart, a maximum power curve can be extracted that determines the flow $q_{t_{MP}}^*$ that gives maximum power output for a target head H^* . Using this maximum power curve, the total optimal flow solution Q_t^* can be allocated to a number of turbines n_{op}^* . Because n_{op} is a discrete variable, and the optimal flow Q_t^* is not necessarily a multiple of $q_{t_{MP}}^*$, the allocated turbine flow q_t^* may not be exactly equal to $q_{t_{MP}}^*$, as illustrated in Figure 5. The flow allocation procedure is shown in the following steps, written in pseudocode:

$Q_t^* \leftarrow$ Total turbine flow solution ;
 $H^* \leftarrow$ Hydraulic head solution ;
 $q_{t_{MP}}^* = q_{t_{MP}}(H^*)$, calculated from maximum power curve in hill chart [13] ;
 $n_{op}^* = \text{ceil}(\frac{Q_t^*}{q_{t_{MP}}^*})$;
 $q_t^* = \frac{Q_t^*}{n_{op}^*}$;
 $\eta^* = \eta(H^*, q_t^*)$.

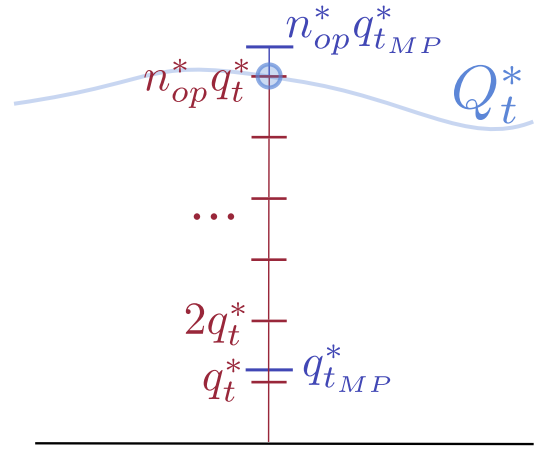


Fig. 5. Representation of the difference between the maximum power flow $q_{t_{MP}}^*$ and the allocated turbine flow q_t^* .

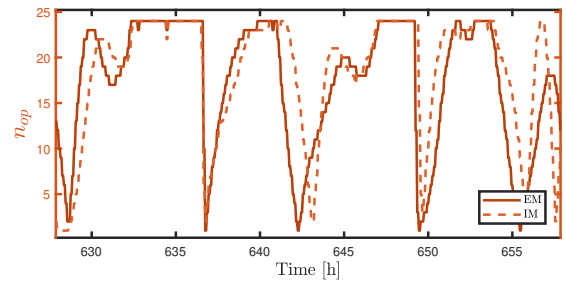


Fig. 6. Number of operating turbines resulting from the optimal control solutions, using the two different objective functions: EM (bold line) and IM (dashed line).

In other words, n_{op}^* turbines operate as close as possible to the maximum power curve, and η^* is extracted from the hill chart for each specific pair (H^*, q_t^*) . It should be noted that using the turbine control allocation algorithm within the controller synthesis procedure (see Section III) would result in a mixed-integer OCP, requiring tailored (and computationally expensive) solvers. Therefore, the implementation of the turbine control allocation algorithm is done *a posteriori*, inevitably resulting in a sub-optimal solution. In other words, the optimal control solution is calculated with the purpose of planning the operation of the barrage and, in a consecutive step, the open-loop turbine control allocation algorithm is used to calculate distribute the optimal turbine flow across the turbines of the barrage.

To illustrate the implementation of the turbine control allocation algorithm, Figure 6 shows the resulting $n_{op}(t)$ of the two objective functions in the winter case during a 30 hour period. It can be seen that, in general, the EM and IM objectives result in similar turbine operation. To approximate the OpEx associated with turbine operation, we consider a constant cost c (in Euro/MW/h) for each hour of operation of each turbine [5]:

$$\text{OpEx} = p_n c \int_{\Omega} n_{op}(t) dt, \quad (24)$$

where p_n is the nominal power of a single turbine (in this case, 10 MW). In this study, a cost $c = 3.72$

TABLE III
OpEx AND REVENUE FOR WINTER AND SUMMER PERIODS

Parameter	Winter period		Summer period	
	EM	IM	EM	IM
OpEx [k Euro]	443	424	413	413
Revenue [k Euro]	4,454	4,637	1,520	1,630

Euro/MW/h is assumed [5]. The revenue is calculated by subtracting costs from income:

$$\text{Revenue} = \text{Income} - \text{OpEx}. \quad (25)$$

As shown in Table III, OpEx, in the winter case with the IM objective, is only around 4% lower than with the EM objective, and negligible in the summer case. This result suggest that, by implementing the IM objective, the turbines are not overutilised, so that the generation periods are shifted, but rather the operation is similar, or even less costly, compared to operation with the EM objective.

V. CONCLUSION

This study utilises different objective functions to optimise the operation of tidal barrages, exploiting the flexibility and energy storage potential of tidal barrage power plants. An income maximisation (IM) objective is shown to effectively increase the revenue of the power plant, compared to an energy maximising (EM) objective function, with an associated decrease in energy generation. As previously mentioned, it is assumed that the controller external inputs (tidal water level and electricity price) exactly resemble those variables in real life. In the case of tidal elevation, although not entirely accurate, using the astronomic tides from the EOT20 is a reliable approximation of the real behaviour of the tidal water level. However, electricity prices are highly volatile and difficult to forecast, which, in practice, could have an impact on the performance of the controller. To address the uncertainty in electricity price, a closed-loop control should be added to feeds real-time information and adapt the optimal trajectories calculated by the controller, which could be considered for future work.

A control allocation algorithm was implemented to distribute the optimal turbine flow between the barrage turbines and estimate an operation and maintenance cost associated with the turbines in service. The results show similar OpEx for both EM and IM strategies, which suggests that an IM objective function does not result in more costly operation of the power plant that could offset the increase in income.

In this study, the OpEx of the turbines is not considered in either of the two objective functions. The moment-based control framework used to solve the OCP of tidal barrages assumes that the solution space of the control and state variables is continuous. More efforts should be put into developing a more sophisticated control strategy in order to include the variable (discrete) number of operating turbines in the power plant model within the controller, which results in a

mixed-integer control problem. This would formulate an objective function that not only accounts for the OpEx of the turbines, but also for start and stop costs, which are indeed relevant [6], and are not considered in this study.

REFERENCES

- [1] A. Skiarski, N. Faedo, and J. V. Ringwood, "Optimisation and control of tidal range power plants operation: Is there scope for further improvement?" *Energy Conversion and Management: X*, vol. 23, p. 100657, Jul. 2024.
- [2] F. Harcourt, A. Angeloudis, and M. D. Piggott, "Utilising the flexible generation potential of tidal range power plants to optimise economic value," *Applied Energy*, vol. 237, no. spatial, pp. 873–884, 2019.
- [3] L. Mackie, F. Harcourt, A. Angeloudis, and M. Piggott, "Income optimisation of a fleet of tidal lagoons," in *Proceedings of the Thirteenth European Wave and Tidal Energy Conference*, Naples, Italy, 2019.
- [4] T. Zhang, C. Williams, R. Ahmadian, and M. Qadrdan, "Optimal Operation of a Tidal Lagoon as a Flexible Source of Electricity," in *2022 IEEE Power & Energy Society General Meeting (PESGM)*, Denver, CO, USA, 2022, pp. 1–5.
- [5] A. Angeloudis, S. C. Kramer, N. Hawkins, and M. D. Piggott, "On the potential of linked-basin tidal power plants: An operational and coastal modelling assessment," *Renewable Energy*, vol. 155, pp. 876–888, 2020.
- [6] B. Bakken and T. Bjorkvoll, "Hydropower unit start-up costs," in *IEEE Power Engineering Society Summer Meeting*, vol. 3, 2002, pp. 1522–1527.
- [7] A. Skiarski, N. Faedo, and J. Ringwood, "Tidal barrage operation optimization using moment-based control," in *Proceedings of the European Wave and Tidal Energy Conference*, vol. 15, 2023. [Online]. Available: <https://submissions.ewtec.org/proc-ewtec/article/view/396>
- [8] —, "Flexible operation of tidal barrages for demand-matching generation: A case study in the La Rance power plant," in *Innovations in Renewable Energies Offshore*, 2024.
- [9] J. V. Ringwood and N. Faedo, "Tidal barrage operational optimisation using wave energy control techniques," *IFAC-PapersOnLine*, vol. 55, no. 31, pp. 148–153, 2022, 14th IFAC Conference on Control Applications in Marine Systems, Robotics, and Vehicles CAMS 2022.
- [10] T. M. Moreira, J. G. de Faria, P. O. V. de Melo, and G. Medeiros-Ribeiro, "Development and validation of an AI-driven model for the La Rance tidal barrage: A generalisable case study," *Applied Energy*, vol. 332, p. 120506, 2023.
- [11] M. G. Hart-Davis, G. Piccioni, D. Dettmering, C. Schwatke, M. Passaro, and F. Seitz, "EOT20: a global ocean tide model from multi-mission satellite altimetry," *Earth System Science Data*, vol. 13, no. 8, pp. 3869–3884, 2021.
- [12] A. Angeloudis, M. Piggott, S. Kramer, A. Avdis, D. Coles, and M. Christou, "Comparison of 0-D, 1-D and 2-D model capabilities for tidal range energy resource assessments," 2017.
- [13] G. Aggidis and O. Feather, "Tidal range turbines and generation on the solway firth," *Renewable Energy*, vol. 43, pp. 9–17, 2012.
- [14] N. Faedo, G. Scarciotti, A. Astolfi, and J. V. Ringwood, "On the approximation of moments for nonlinear systems," *IEEE Transactions on Automatic Control*, vol. 66, no. 11, pp. 5538–5545, 2021.
- [15] —, "Energy-maximising control of wave energy converters using a moment-domain representation," *Control Engineering Practice*, vol. 81, pp. 85–96, 2018.
- [16] N. Faedo, G. Scarciotti, A. Astolfi, and J. V. Ringwood, "Non-linear energy-maximizing optimal control of wave energy systems: A moment-based approach," *IEEE Transactions on Control Systems Technology*, vol. 29, no. 6, pp. 2533–2547, 2021.
- [17] EMBER, "European wholesale electricity price data," 2024, Accessed in February 2025. [Online]. Available: <https://ember-climate.org/data-catalogue/european-wholesale-electricity-price-data/>